



TITLE:

Estimation of Remaining Strength of Steel Wire Rope by Electromagnetic Testing

AUTHOR(S):

HANASAKI, Koichi; TSUKADA, Kazuhiko; FUJINAKA, Yuzo; TASHIMO, Kazuo

CITATION:

HANASAKI, Koichi ...[et al]. Estimation of Remaining Strength of Steel Wire Rope by Electromagnetic Testing. *Memoirs of the Faculty of Engineering, Kyoto University* 1991, 53(4): 215-235

ISSUE DATE:

1991-10-31

URL:

<http://hdl.handle.net/2433/281445>

RIGHT:

Estimation of Remaining Strength of Steel Wire Rope by Electromagnetic Testing

By

Koichi HANASAKI*, Kazuhiko TSUKADA*, YUZO FUJINAKA**
and Kazuo TASHIMO***

(Received June 24, 1991)

Abstract

Two methods to estimate remaining strength of steel wire ropes on site by electromagnetic testing data are described.

One is for winding ropes of inclined shafts in a coal mine ; the remaining rope strength (F_R) is given by $F_R = F_0 B^{-m}$, where F_0 is the initial strength, B is the background noise level on a recording chart and m is a constant which depends on the shaft.

The other is for parallel wire stand ropes which are used as tension members of a suspension roofing ; the remaining rope strength can be computed using the cross sectional area loss which is estimated from the electromagnetic testing records.

1. Introduction

Electromagnetic testing of wire ropes is normally used for detecting defects derived from broken wires, spotty corrosion or localized wear by reading deflections recorded on a chart, which may contain much useful information on the rope deterioration. Two methods to estimate remaining strength are described here as follows :

(1) After a breaking test of several winding ropes removed from four inclined shafts of a coal mine, it was found that background noise level, or base line thickness, observed on the recording charts of electromagnetic testing, relates exponentially to the remaining strength unless any broken wire is included, and that characteristics of the relation depend on the shaft conditions because the noise level can be considered to represent the magnitude and the density of the minute imprints on wires which are caused by frequent alternations of bending and tension during the long service period¹⁻²⁾.

(2) Large-diameter wire ropes are used as major elements in suspension roofings

* Department of Mineral Science and Technology

** Fukui Institute of Technology (Professor Emeritus)

*** Hokkaigakuen Kitami University

or in suspension bridges, and long-term exposure to weather conditions deteriorate them by corrosion internally rather than on the surface. There has been a great need to evaluate this deterioration to decide whether they require replacement. Some electromagnetic inspection instruments are available mainly for wire strand ropes which move, such as mine hoisting ropes³⁻⁵). However, for large-diameter stationary ropes, such as suspension cables and mooring cables, there is no equipment available for inspection work, and no prior experience in this area outside of visual examination.

The authors developed two electromagnetic testing instruments, one for Parallel Wire Strand (P. W. S.) suspension cables up to 50 mm in diameter and the other for those up to 85 mm in diameter⁶). These instruments have two main features: (i) flux inspection sensitivity is independent of the relative rope speed, as required for inspecting stationary rope, and (ii) they are able to detect cross sectional location of defects. Using these instruments, the authors inspected P.W.S. cable which had been seriously corroded in an open-air suspension roofing building, and then they evaluated the deterioration of the ropes through laboratory calibration in terms of the loss in the cross sectional area, by a method similar to Bergander's⁷).

In general, it is not easy to estimate the remaining strength of ropes immediately from the loss in the cross sectional area. This is due to the fact that the quality of the defect and the original structure of the rope also affect the remaining strength. The simpler construction of P.W.S. compared with ordinary twisted ropes makes its mechanical behavior less complicated. Therefore, the remaining strength of P.W.S. can be estimated simply by a numerical simulation if the extent of the defect in the rope is known, i.e., the loss in the cross sectional area⁸).

2. Estimation of Remaining Strength of Haulage Ropes

This section describes the relation between the remaining rope strength measured by a breaking test and the background noise level on the record chart obtained by an electromagnetic test. Moreover, the authors propose a new useful nomograph for rope maintenance in an inclined shaft.

2.1 Field Tests and Breaking Tests

Table 1 shows the dimensions of inclined shafts and their winding rope systems investigated by an electromagnetic instrument. All ropes had served hoisting for so long a time under different conditions that they might have their own characteristics of deterioration⁹).

Table 1. Dimensions of inclined shafts and the winding ropes.

Shaft/Rope	A	B	C	D
Winding System	Single drum	Single drum	Tandem driven Koepe	Single drum
Conditions*	U (C)	U (C/P)	U (P)	S (D)
Rope travel (m)	1,057	2,800	621	600
Winding drum dia. vs. outlayer wire dia.	649	663	765	584
Winding rope				
Construction	6×F(16)	6×7**	6×7**	6×7**
Diameter (mm)	33.5	35.5	35.5	28.0
Elapsed time (month)	33	11	53	51
Total count of winding	39,420	5,650	121,293	27,307

* U: Underground, S: Surface, C: Coal, P: Personnel, D: Debris.

** Shaped wire.

Figures 1,2,3 and 4 are the electromagnetic testing charts recorded from the ropes in the inclined Shafts A,B,C and D respectively, immediately before their removal for replacement. Each chart was obtained by a DC electromagnetic instrument with a search coil located at a point in the inclined shaft where the longest portion of the rope could be tested. The instrument's sensitivity was calibrated by the deflection of on the chart when detecting a piece of wire attached on the surface of the rope.

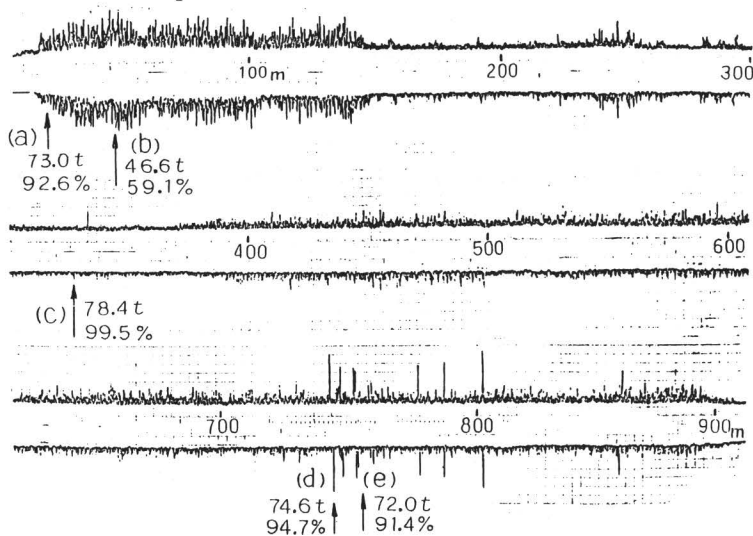


Figure 1. The electromagnetic inspection record of the winding rope in the inclined shaft A. Arrows show the breaking test sample locations.

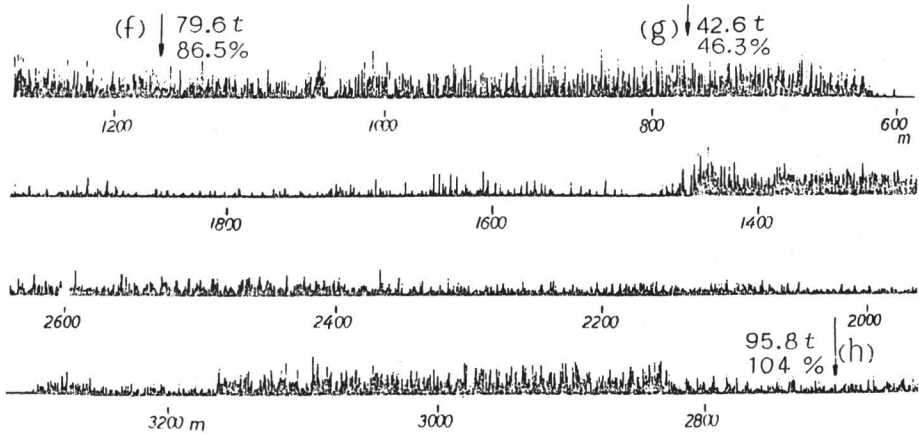


Figure 2. The electromagnetic inspection record of the winding rope in the inclined shaft B. Arrows show the breaking test sample locations.

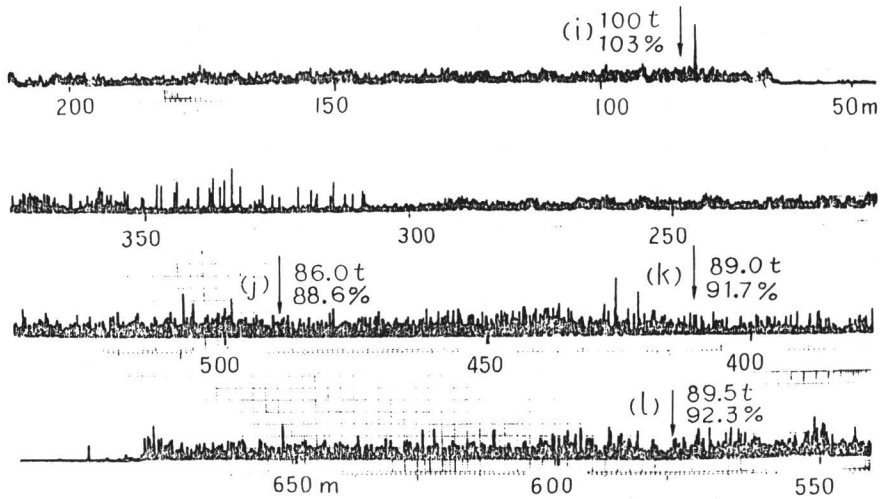


Figure 3. The electromagnetic inspection record of the winding rope in the inclined shaft C. Arrows show the breaking test sample locations.

According to the records in these figures, several specimens for breaking tests were extracted after their removal for replacement from sections having different deterioration levels in each rope. Locations of the specimens are shown by the alphabetical marks with an arrow such as (a), (b), ... and (s) in Figures 1, 2, 3 and 4.

2.2 Background Noise Level of Record and Remaining Strength

Remaining strength of specimens (F_R) measured by breaking tests are plotted

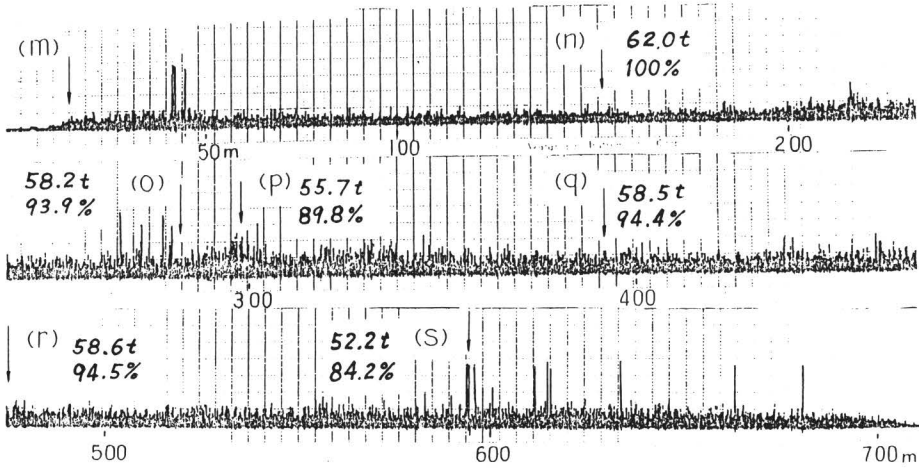


Figure 4. The electromagnetic inspection record of the winding rope in the inclined shaft D. Arrows show the breaking test sample locations.

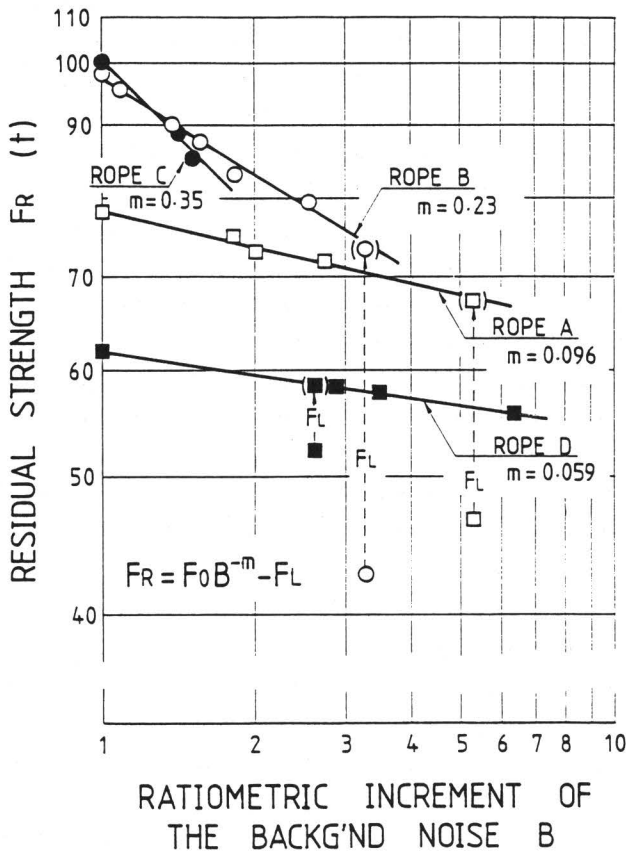


Figure 5. Remaining rope strength (F_R) measured by breaking test vs. ratiometric increment of the average background noise level (B) observed on the inspection records.

against the background noise level ratio (B) between at the end of the service life and the beginning of the service life on a log-log scale chart as in Figure 5. The intact rope strength of each shaft (F_0) is dotted on the left edge of the graph (i.e. $B = 1$). Data for each rope falls on its specific straight line: except in case any broken wire is included in the specimen, the following relation can be derived:

$$F_R = F_0 B^{-m} \quad (1)$$

where m is a constant value depending on the conditions of the shaft where the rope was.

If some broken wires exist in that portion, the remaining strength is corrected by the strength loss (F_L) due to the breakage, that is:

$$F_R = F_0 B^{-m} - F_L \quad (2)$$

Regarding the value m , the 0.0966 of Rope A and 0.059 of Rope D are very different from the 0.25 of Rope B and 0.35 of Rope C. Since Ropes B, C and D have the same construction, 6×7 , and differ from Rope A as shown in Table 1, the difference of the value m between Ropes A and D and Ropes B and C is not considered to derive only from their constructions but also from the shaft conditions. As the atmospheres in the tunnels of Shafts A and D are reported to be much dryer than those in Shafts B and C, Ropes A and D must have been deteriorated only outside, by physical causes such as abrasion by friction or metal fatigue by alternating stresses. On the other hand, since Rope B has been used where a lot of corrosive water is flowing over the floor, and Rope C was affected by the damp air in the inclined shaft, those ropes must have badly corroded inside. These situations must be the reasons why the decreases in strength of Ropes B and D are so much greater than those of Ropes A and C in spite of the relatively small background noise level. Therefore, the value m can be considered as an index for the characteristic of each winding system, that is, the value m represents the deterioration tendency that depends on the conditions of the system as well as the environment of the shaft.

2.3 Nomograph for Rope Maintenance

As described in the last section, the remaining rope strength can be estimated by the background noise level of the base line on the electromagnetic testing chart, and the relationship between them is considered to be a characteristic of the rope winding system in the shaft¹⁰⁾.

Once a characteristic relation as expressed in Eq. (1) is obtained for the first generation rope for a shaft, that is, the value m and the initial strength F_0 are known,

the relation will be applicable to the second generation rope and also to the subsequent ropes unless the shaft conditions change drastically. Moreover, if background noise levels on the base line vs. duration of the first generation rope are recorded for its service life, a nomograph for rope maintenance can be drawn.

Figure 6. is an example of the nomograph for a vertical shaft with a haulage rope : 54 mm diameter, $195 + 8 \times F(10)$ and 207 tons of intact rope strength. Curve (1) shows how background noise levels on the base line of the electromagnetic testing record increase with the duration of use (months) from the date of installation to the date of retirement. Curve (2) shows the haulage plan expressed by the number of months and the number of times of hoisting. Curve (4) shows the relation between the results of breaking tests of several specimens having different degrees of deterioration and background noise levels on the base line as expressed by Eq. (1). Thus, Curve (3), which shows the remaining strength at any time of

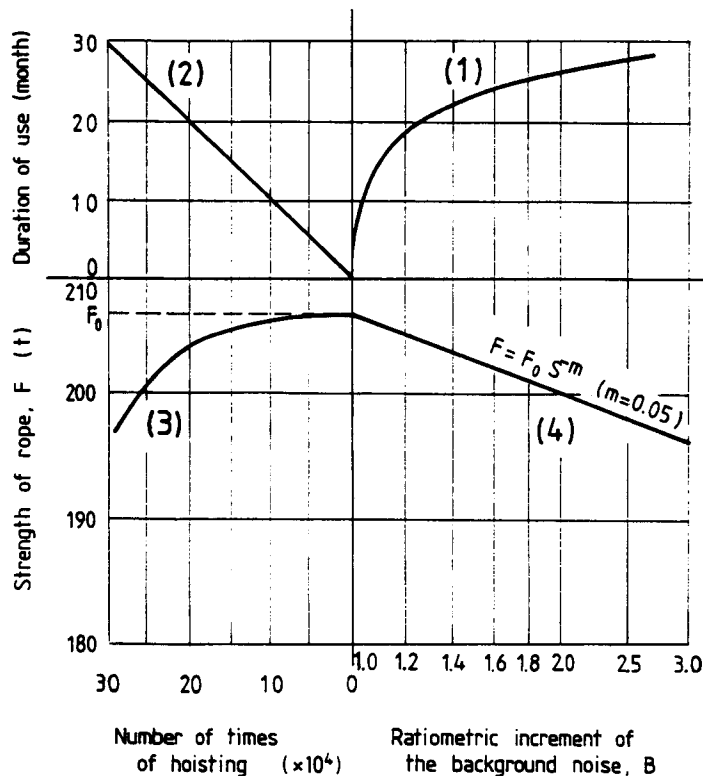


Figure 6. Nomographic chart useful for the winding rope maintenance of a vertical shaft. Relations among the duration of use, the times of hoisting, the background noise on the electromagnetic testing record, and remaining rope strength are easily obtained from this figure.

hoisting, is derived from the other three curves. If some breakages of wire are predicted by the field electromagnetic testing, Curves (3) and (4) should be shifted downward by the amount corresponding to strength loss (F_L) as shown in Eq.(2). Therefore, the relation between the amount of strength loss and the signal level of the broken wire must be determined in advance or at the first rope retirement by breaking tests with specimens which have some broken wires. For describing the rope maintenance usage of this figure, since Curve (2) is determined as the haulage plan of the shaft, the relation between the duration of use or number of times of hoisting and the strength loss can be estimated from Curve (1) and (4): and then, if a limit of strength (derived from a safety factor) is set on Curve (3), it is possible to estimate how long the rope can serve in the shaft.

3. Estimation of Remaining Strength of Corroded P.W.S. Cables

This section describes in detail these newly developed electromagnetic testing instruments. The electromagnetic testing carried out to estimate the degree of corrosion in P.W.S. cables of a suspension roofing, and the estimation of the remaining strength of P.W.S. from inspection records are also described.

3.1 New Electromagnetic Testing Method Applied to P.W.S. Cables

3.1.1 P. W. S Cable

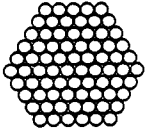
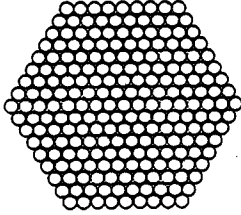
P. W. S. cables, constructed of a hexagonal bunch of 30–300 wires, are used as major elements in suspension roofings and suspension bridges. Because the individual wire of a P. W. S. is not twisted, P. W. S. cables have high strength and become less elongated than ordinary twisted ropes when subjected to a tensile load. These features of P. W. S. cables make them suitable for use as suspension cables. However, their drawback is that they tend to corrode internally. Table 2 shows the properties and cross section of a P. W. S. 75 and a P. W. S. 217, which the authors inspected in the field.

3.1.2 Construction of Testing Instruments

For the inspection of corroded P.W.S. suspension cables, the authors manufactured two instruments, each of which consists of a DC electromagnetic exciter and a leakage flux detector. These are different in the method of rope magnetization. As shown in Figures 7(a) and 7(b), one is a yoke type, and the other is a solenoid type. The yoke type instrument utilizes an electromagnet which produces longitudinal magnetic field in the rope between two poles. The other instrument utilizes two solenoidal coils coaxial with the rope for the magnetization. Though the solenoid type instrument has the inconvenience of

Table 2. Specifications of P. W. S. cables.

Parallel Wire Strand	P. W. S. 75	P. W. S. 217
Number of component wires	75	217
Cross sectional area	1,473 mm ²	4,261 mm ²
Nominal breaking strength	224 tonf	648 tonf
Weight per length	11.5 kgf/m	33.4 kgf/m

Cross sectional view		
----------------------	---	--

Component wire	
Diameter	5.0 mm
Elastic modulus	19,900 kgf/mm ²
Tensile strength	166 kgf/mm ²

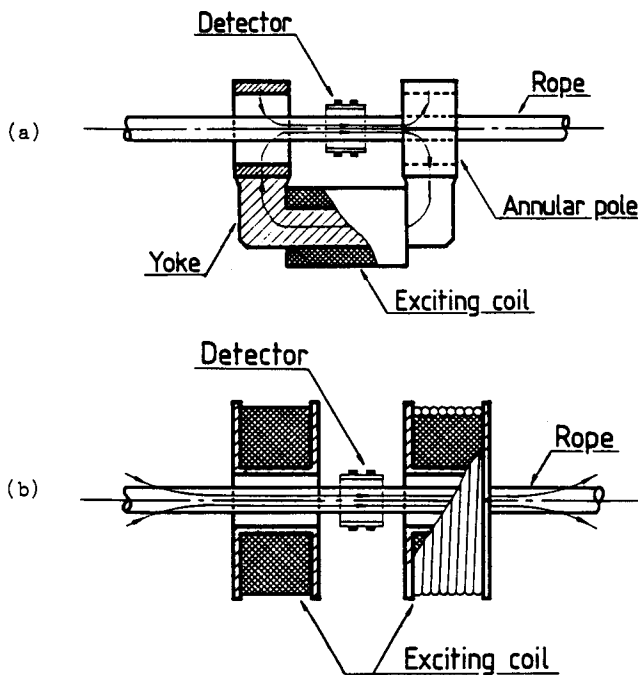


Figure 7. Testing instruments for P.W.S. cables.

(a) Yoke type instrument.

(b) Solenoid type instrument.

coiling up the conductor around the rope for each test, it has some advantages, especially to inspect large-diameter ropes such as P.W.S. 217 cables; for instance: i) the instrument is lighter than that of the yoke type due to the absence of iron core and yoke, ii) the magnetic field induced by the solenoidal coils is relatively uniform, and consequently, the difference between the inspection sensitivity of a defect in the surface and that of an inner one is relatively small. The yoke type instrument and the solenoid type instrument were used for the field tests of P.W.S. 75 and P.W.S. 217 cables, respectively.

The detector unit, shown in Figure 8, has twin annular arrays of Hall effect elements attached on the circumference of the divided pipe: it senses only the radial component of the leakage flux produced by localized defects in the P.W.S. This detector unit has two main features. The first feature is that the sensitivity of detecting defects in a rope is independent of the relative rope speed, as required for inspection of stationary ropes such as suspension cables. This sensitivity is achieved by the use of the Hall effect element in this detector unit. The second feature is that the detector is able to locate a defect in the cross section of a rope. As can be seen in Figure 8, each annular array is divided into 6 segments. These segments establish the omnidirectional sensitivity of the detector unit. Furthermore, the individual output of segments can be extracted in order to locate the defect in the cross section.

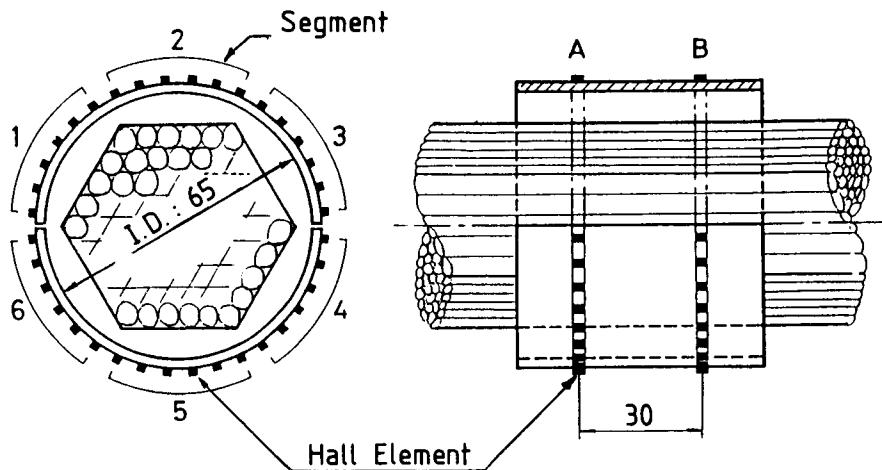


Figure 8. Leakage flux detector (for P.W.S. 75).

3.1.3 Interpretation Method of Inspection Records

To interpret the records (a sample is shown in Figure 9), the height (H) of the deflection and the width (W) of the deflection at the base are taken into

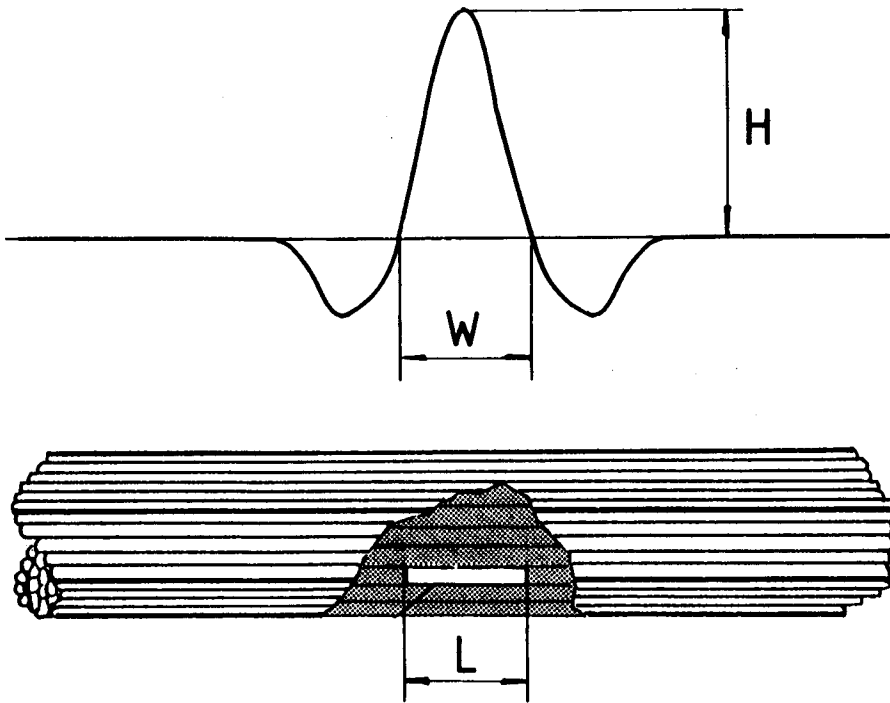


Figure 9. Typical signal related to a defect.

consideration. While the width of the deflection is closely related to the defect length (L), the height is related to the loss in the cross sectional area of the defect. However, a defect in the surface of the rope will cause a greater height deflection than the same defect in the inner part of the rope. In other words, the sensitivity of the detector is affected by the location of the defect in the cross section. Figure 10(a) shows the detector sensitivity as a function of defect location (one broken wire) in different parts of the cross section. This varying sensitivity introduces error in the evaluation of the inspection records. Therefore, in order to interpret the inspection records accurately, the location of the defect in the cross section must be known. To do this, the authors utilized a detector head divided into 6 segments.

Figure 10(b) shows the sensitivity of the detector in which one segment of the annular array is active. This monodirectional sensitivity chart is useful to locate the rope cross section. Measuring the heights ($H_1 \sim H_6$) of the deflections on six monodirectional inspection records, and making a hexagonal chart as illustrated in Figure 11, the defect can be roughly located.

The procedure with which the authors evaluated the extent of a defect is as

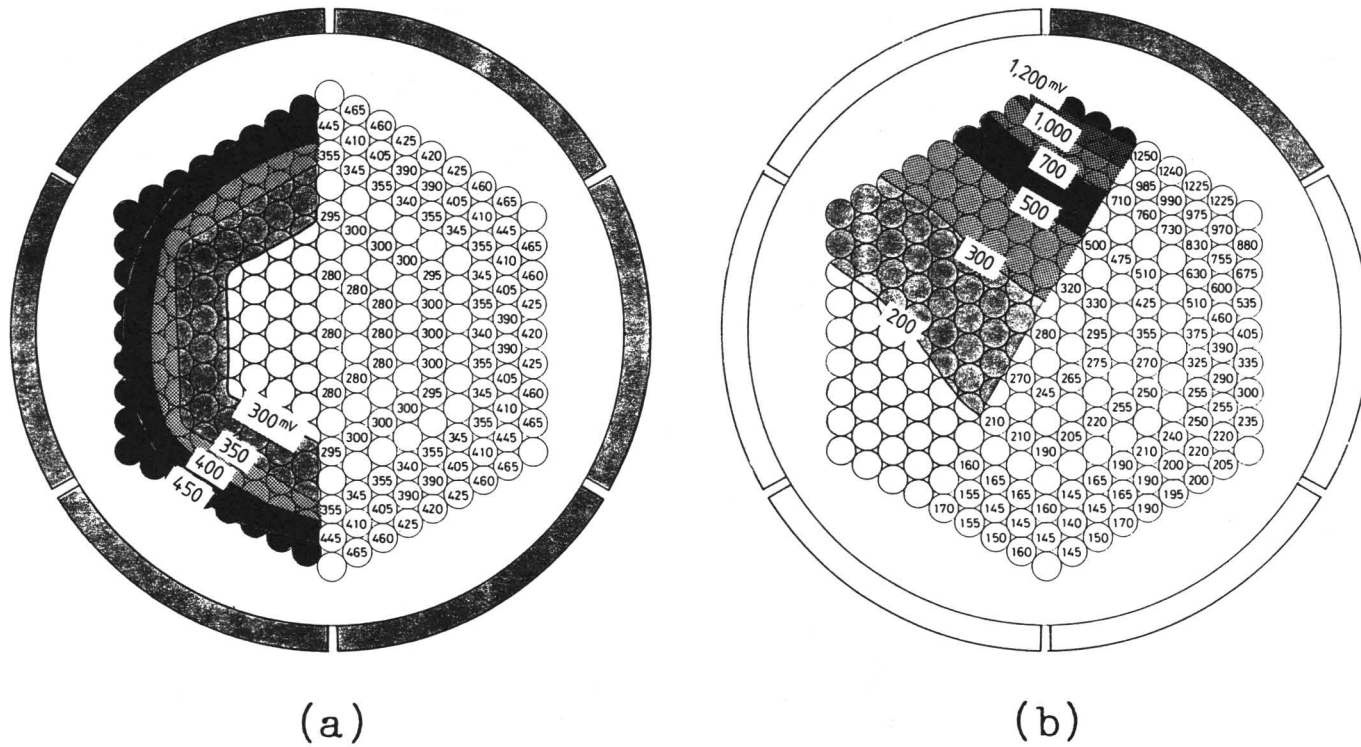


Figure 10. Detector sensitivity as a function of defect location in different parts of the cross section (smudged segment(s) on active).
 (a) Omnidirectional inspection.
 (b) Monodirectional inspection.

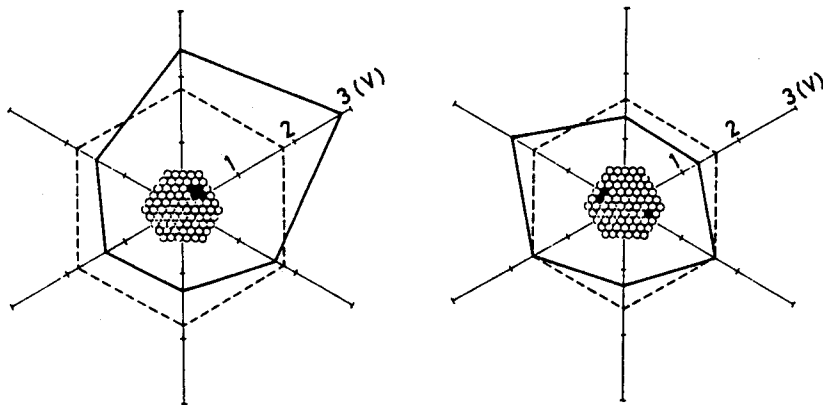


Figure 11. Examples of Hexagonal chart showing the output voltage from each detector segment.

follows:

- i) measuring the height (H) and the width (W) of the record on the omnidirectional inspection chart,
- ii) deciding the gap length (G_{eq}) of an imitated broken wire which presents a deflection of the same width (W),
- iii) measuring the sensitivity as a function of defect location in the cross section, using the imitated broken wire whose gap length is equal to G_{eq} (cf. Figure 10 (a)),
- iv) making a hexagonal chart from the six monodirectional inspection records (cf.

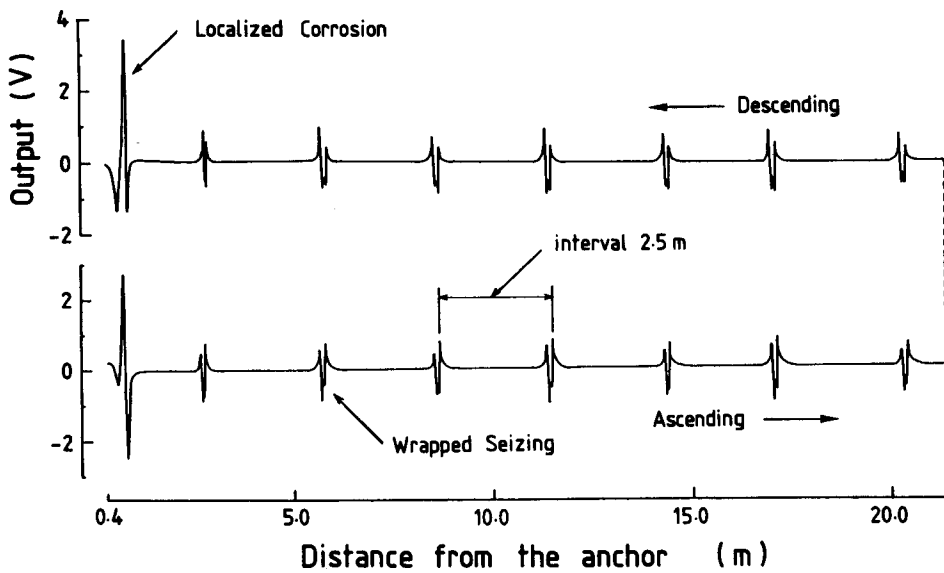


Figure 12. Inspection record of a P.W.S. 75.

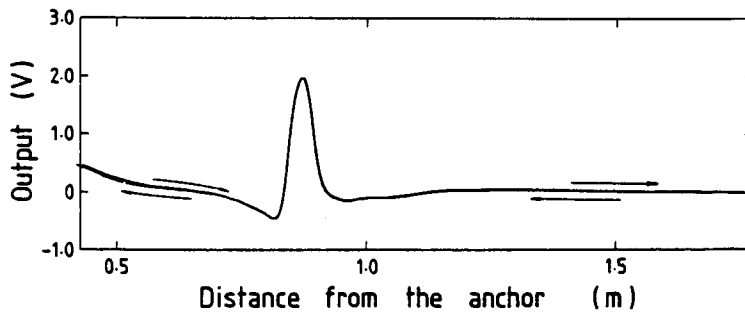
Figure 11),

v) the extent of the defect can be evaluated in terms of the loss in cross sectional area from the height of the deflection (H) with the figure of the sensitivity and the hexagonal chart.

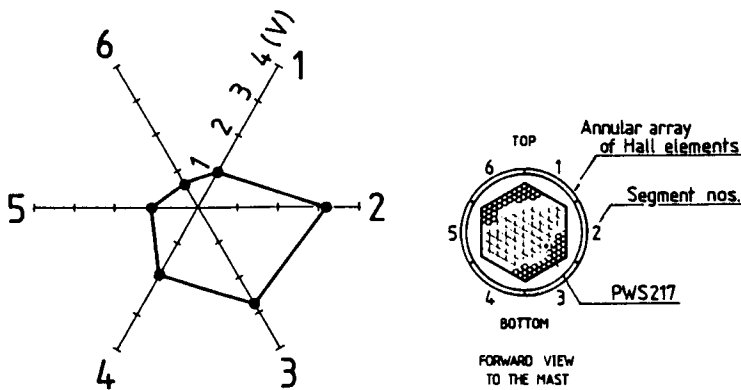
3.1.4 Field Test

The instruments were used to evaluate the deterioration of P.W.S. 75 and P.W.S. 217 cables which had been used in a suspension roofing. These P.W.S. cables had been seriously corroded in a limited portion near the anchor after 15 years of usage. The corrosion occurred just above a 1 m greased section connected to the anchor. Thirty two suspension cables (twenty two P.W.S. 75s and ten P.W.S. 217s) were inspected on this suspension roofing.

Figure 12 shows a typical recording chart of these P.W.S. 75 cables. Both the ascending and descending record are graphed in the same figure. A localized sharp



(a)



(b)

Figure 13. Examples of inspection charts of a P.W.S. 217.

(a) Omnidirectional inspection record.

(b) Hexagonal chart.

deflection on the left end of the chart in Figure 6 indicates a badly localized corrosion defect as confirmed by visual examination. The similar shaped smaller downward deflections indicate not defects but the wire wrappings located at intervals of 2.5 m along the P.W.S. There seem to be no defects in other parts of the P.W.S.

Figure 13(a) shows the omnidirectional inspection chart along the P.W.S. 217 cable up to 1.8 m from the anchor. The deflection at 0.9 m on the chart indicates a localized corrosion defect. Figure 13(b) shows the hexagonal chart obtained from six monodirectional inspection records which suggests that the defect would be in the lower right-hand part of the cable cross section.

Every rope in this field had a similar deterioration similar to the above examples. Two P.W.S. 75 cables which were most seriously corroded were evaluated to have a 19.5 – 30.1 % loss and a 10.0 – 20.0 % loss in cross sectional area of the corroded part, respectively. In view of this evaluation, these cables were replaced for fear that the actual strength reductions might be much higher than the area losses.

3.2 Examination of P.W.S. Cables Removed for Replacement

3.2.1 Tensile Breaking Test

A 4 m-long sample, including a portion of sharp localized corrosion, was cut out of each of the two removed P.W.S. 75 cables, and one more sample was cut out of the portion which seemed to have no corrosion. These three samples were subject to a tensile breaking test. Figure 14 shows the load-deformation characteristics of these two corroded samples (No. 2, 3) and the non-corroded sample (No. 1).

In the breaking test of corroded sample (No. 3), one individual wire broke first at a load of 64 tons, and then 21 wires broke progressively up to the maximum load, as confirmed by sudden decreases of the load, that is, discontinuity of the load deformation curve in Figure 14, as well as by the audio sound of the breaks. The samples (No. 2, 3) which had localized corrosion presented unique deformation behavior similar to brittle materials; this was in contrast to the non-corroded sample (No. 1) which showed normal elasto-plastic behavior. This unique behavior suggests that the P.W.S. is a bunch of wires corroded to various degrees. The breaking strengths of the corroded samples (No. 2, 3) were 146.5 tons (67 % of the nominal tensile strength) and 126.5 tons (56 %), respectively, and that of the non-corroded sample was 238.5 tons (106 %).

3.2.2 Disassembly of the Corroded P.W.S. Sample

After the breaking test, the corroded P.W.S. sample (No. 3) was disassembled, and the individual wires were observed. Corrosion was localized within the range

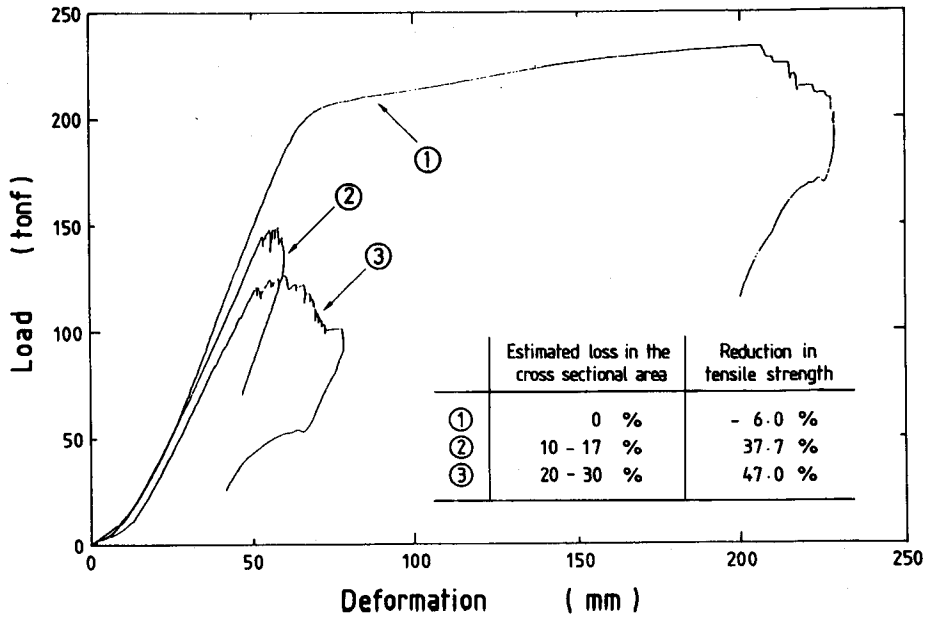


Figure 14. Load-deformation characteristics of three removed P.W.S. 75s.

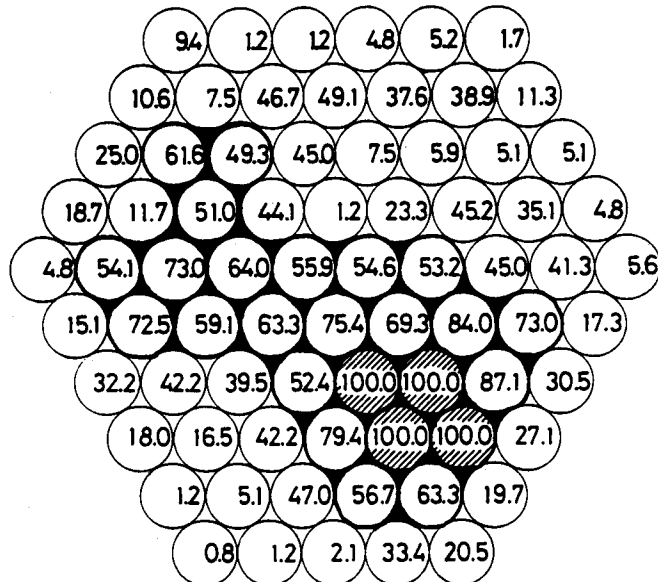


Figure 15. Cross sectional area loss in percent of each individual wire of a removed P.W.S. 75.

Black zone : over 50% loss.
 Hatched wire : broken completely.

of 600 – 750mm from the anchor. Four component wires had been broken by corrosion before the breaking test.

The maximum cross sectional area loss of each component wire, obtained by measuring the minimum diameter of each wire, is shown in Figure 15. The inner wires were more seriously corroded than the surface wires, which suggests that water is prone to accumulate inside the P.W.S. The maximum total area loss in cross section of the P.W.S. 75 was 22.8 % at 650 mm from the anchor. Considering that the individual wires had been elongated and had become thinner to a certain degree through the breaking test, the actual area loss was estimated to be about 20 %, corroborating the result of the electromagnetic inspection.

3.3 Estimation of Remaining Strength by Numerical Simulation

The actual remaining strength of the corroded P.W.S. was considerably lower than expected from the area loss in it . This seems to be caused by the fact that the P.W.S. was a bunch of wires corroded to various degrees. In order to estimate the remaining strength of the P.W.S. with localized corrosion, the authors carried out a numerical simulation on the load-deformation characteristics of corroded P.W.S. , based on the cross sectional area loss estimated by the previous electromagnetic testing.

3.3.1 Procedure

The following assumptions were used for the simulation :

i) Properties of corroded individual wires

An individual corroded wire was assumed to be shaped as shown in Figure 16, where L is the wire length, ηL is the corroded portion length, A is a cross sectional area of the intact wire and ξA is that of the corroded portion. Each wire was assumed to behave elastically until the stress reached the tensile strength of the wire, and at that point to break completely. The elastic modulus or Young’s modulus (E) of the wires is assumed not to change in spite of corrosion. Stress distribution is uniform and in proportion to the ratio of the cross sectional area: stress in the corroded portion (I in Figure 16) is higher than that in the non-corroded portion (II in Figure 16). Stress in the corroded portion (σ_I) and the non-corroded portion (σ_{II}) are expressed in Eq. (3) and Eq. (4).

$$\sigma_I = \frac{E}{\xi - \xi\eta + \eta} \cdot \bar{\epsilon} \quad (\bar{\epsilon}: \text{total strain of a wire}) \quad (3)$$

$$\sigma_{II} = \begin{cases} \xi \sigma_I & (\sigma_I \leq S_t) \\ 0 & (\sigma_I > S_t) \end{cases} \quad (4)$$

The strength of a wire is assumed to hold the nominal tensile strength until it

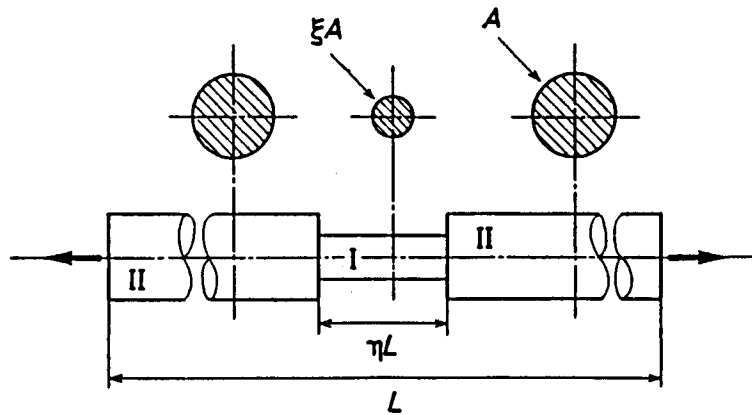


Figure 16. Model of an individual corroded locally.

breaks: in other words, it is assumed to break when the stress in the corroded portion of the wire (σ_c) reaches the nominal strength (S_t).

ii) Cross sectional area loss of individual wires

For the simulation, we need to assume a cross sectional area loss of each individual wire that has been corroded to a different degree. In other words, we need to prepare a value (ξ) for each wire in Eq. (3). The measured area losses of 75 individual wires are indicated as black dots in Figure 17, arranged in order of least loss. It seems to be questionable that these values are equal to the actual area loss in the field because they were measured after the breaking test in the laboratory. The distribution of the area loss in individual wires seems to be common to all P.W.S. in the suspension roofing examined. Therefore, we assume that the cross sectional area loss of each individual wire is as indicated by the broken lines in Figure 17: three types were selected having total P.W.S. area losses of 30%, 20% and 10%. During the simulation, the strain ($\bar{\epsilon}$) was gradually increased by steps of 0.01% and the bearing load calculated for each step according to Eq. (3) and Eq. (4) with $E = 19,900 \text{ kgf/mm}^2$, $S_t = 166 \text{ kgf/mm}^2$, $L = 4,000 \text{ mm}$ and $\eta L = 150 \text{ mm}$.

3.3.2 Results

Figure 18 shows the simulated load-strain characteristics of three corroded P.W.S. 75 cables. If the area loss of a P.W.S. was 10%, 20% or 30%, the remaining strength would be 69%, 52% or 38%, respectively. As shown in the same figure, the load-strain curve of a P.W.S. with 20% area loss in cross section is recognized to correspond closely to the actual deformation curve of the corroded P.W.S. 75 (No. 3) in Figure 14. This suggests that the simulation is acceptable for the evaluation of the remaining strength of P.W.S. The results of the simulation

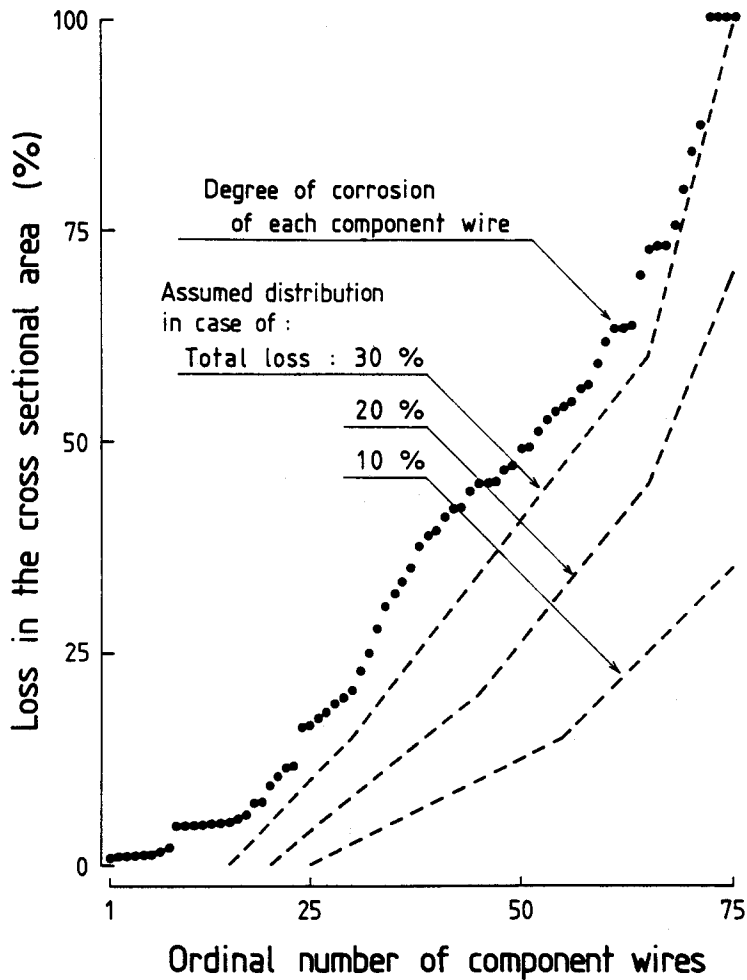


Figure 17. Distribution of the measured area loss and assumed area loss of individual wires used for a numerical simulation.

Table 3. Estimated remaining strength of P. W. S.

Estimated cross sectional area loss	Decrease in tensile strength	
	calculated	measured
10-17%	30-43%	37%
20-30%	48-59%	47%

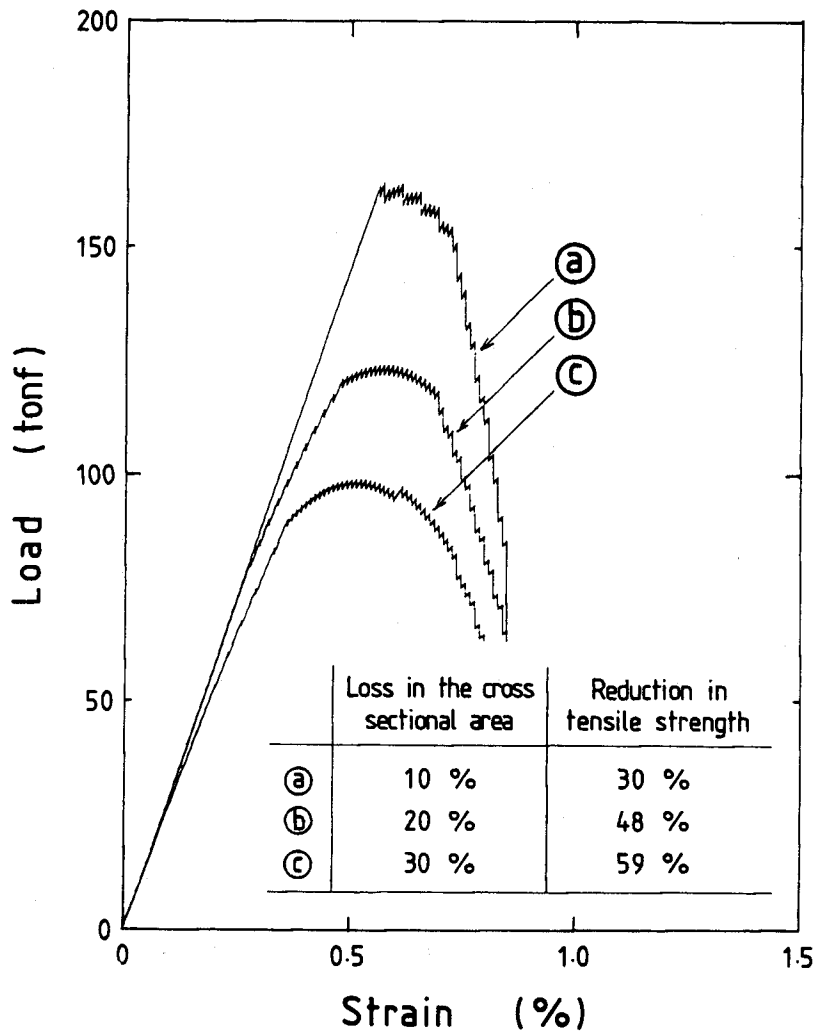


Figure 18. Calculated load-strain characteristics of three corroded P.W.S. 75s.

are summarized in Table 3, which shows the remaining rope strength calculated from estimated area loss in comparison with the real strength.

4. Conclusions

(I) Hauling rope

The background noise level, or base line thickness in plain words, observed on the electromagnetic testing record represents the degree of deterioration of the rope

because it is considered to be derived from the magnitude and density of the minute imprints on the wires, which are caused by frequent alternations of bending and tension level through the service period. Moreover, from the results of breaking tests with rope specimens having different degrees of deterioration, the background noise level (B) relates to the remaining strength of the rope (F_R) as $F_R = F_0 B^{-m}$, where m is a characteristic constant depending on the field conditions of the shaft, F_0 is the initial strength of the rope depending on the construction. A nomograph which can be drawn by using the above relation, the field testing records during the service life, and the haulage plan of the shaft are helpful for maintenance of the second and the subsequent rope.

(II) Suspension cable

New electromagnetic testing instruments were developed to evaluate the deterioration of P. W. S. cables. It was found that these instruments are suitable for inspecting the deterioration of suspension cables such as P.W.S. cables in suspension roofings. Furthermore, through the experimental investigations and the numerical simulations, the following points were noted: (i) The cross sectional area loss estimated by electromagnetic testing corresponded closely to the actual area loss in P. W. S. cables examined in the field. (ii) Although the actual remaining strength of a P. W. S. is much lower than expected from the area loss, this can be estimated by numerical simulation due to the simple construction of P. W. S. cables.

References

- 1) K. Tashimo, J. Kokado and Y. Fujinaka, *Mining and Metallurgical Ins. of Japan*, **89**, 1030, pp. 287–292 (1979).
- 2) H. Arnold, *Glückauf*, **110**, 11, pp. 435–439 (1974).
- 3) J. G. Lang, *Proc. of the 70th Annual Meeting of CIMM (Vancouver, April 1968)*, pp. 1–10.
- 4) D. N. Poffenroth, *Proc. 1979 ASNT/CSNDT Conference (Niagara Falls, NY, 1979)*, pp. 1–19.
- 5) H. R. Weischedel, *Materials Evaluation*, **43**, pp. 1592–1605 (1985).
- 6) Y. Fujinaka, K. Hanasaki and K. Tsukada, *Mining and Metallurgical Ins. of Japan*, **102**, 1185, pp. 783–788 (1986).
- 7) M. J. Bergander, *Int. Adv. in Nondestructive Testing*, **9**, pp. 113–123 (1983).
- 8) Y. Fujinaka, K. Hanasaki, K. Tsukada, N. Yoshioka and K. Sugii, *Proc. of 11th WCNDT*, **1** (1985), pp. 154–161.
- 9) K. Tashimo, J. Kokado, Y. Fujinaka, H. Nohara and Y. Kondo, *Mining and Metallurgical Ins. of Japan*, **95**, 1093, pp. 143–148, (1979).
- 10) K. Tashimo, J. Kokado, Y. Fujinaka and S. Nishikiori, *Mining and Metallurgical Ins. of Japan*, **91**, 1047, pp. 335–339 (1975).